



OPEN

# Pd on thermo-responsive composite of silica-coated carbon nanotube and 1-vinyl-3-butylimidazolium-based ionic liquid copolymers as an efficient catalyst for hydrogenation of nitro compounds

Samahe Sadjadi<sup>1</sup>✉, Neda Abedian-Dehaghani<sup>2</sup> & Majid M. Heravi<sup>2</sup>✉

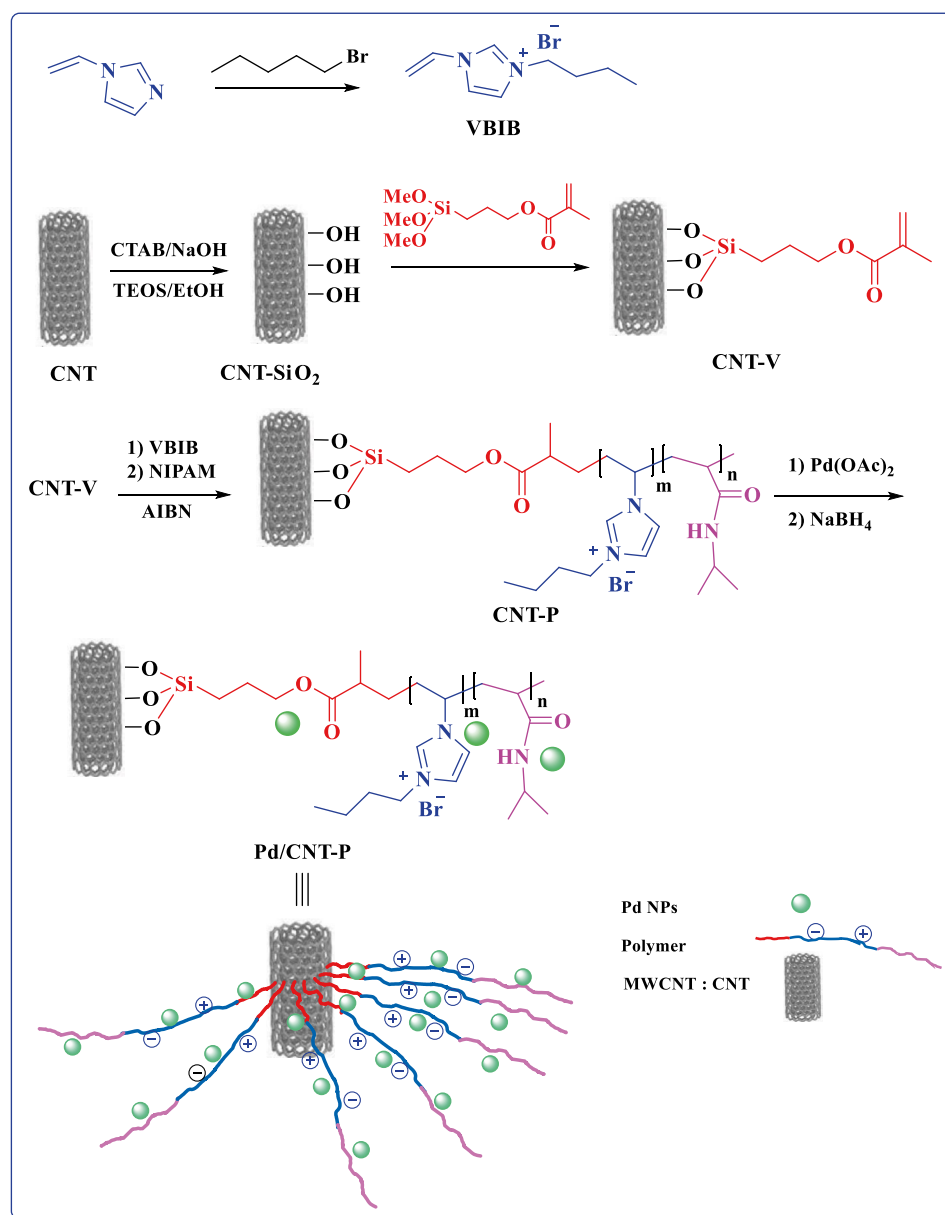
In this work, an ionic liquid-containing thermo-responsive heterogeneous catalyst with utility for promoting hydrogenation of nitro-compounds in aqueous media is developed. To prepare the catalyst, silica-coated carbon nanotubes were synthesized and vinyl-functionalized. The resulted compound was then polymerized with 1-vinyl-3-butylimidazolium bromide and *N*-isopropylacrylamide. The obtained ionic liquid-containing thermo-responsive composite was palladated via wet-impregnation method to give the final catalyst. Study of the performance of the catalyst confirmed high catalytic activity of the catalyst at temperature above the lower critical solution temperature. Furthermore, the catalyst was highly recyclable and showed negligible Pd leaching upon recycling. Broad substrate scope and selectivity of the catalyst towards reduction of nitro functionality were also confirmed. Furthermore, hot filtration test implied the heterogeneous nature of the catalysis. The comparison of the activity of Pd/CNT-P with some control catalysts approved the importance of hybridization of P and CNT and the presence of ionic liquid for the catalytic activity.

Smart polymers are polymeric compounds<sup>1–3</sup> that respond to the external stimuli, such as mechanical force, light<sup>4</sup>, temperature<sup>5,6</sup>, pH<sup>7</sup> etc. This class of polymers has gained considerable attention and has been successfully applied in diverse range of applications, including catalysis, thermochromic and electrochromic materials, biomedical fields, matrix chemistry, etc<sup>8,9</sup>. Poly (*N*-isopropylacrylamide), PNIPAM, is a well-known thermo-responsive polymer that in response to temperature can generate a phase-separation in the aqueous solution at the lower critical solution temperature (LCST)<sup>10</sup>. In fact, the hydrogen bonds between this polymer and water can result in dehydration and phase separation<sup>10,11</sup>.

Among various carbon nanomaterials, carbon nanotubes<sup>12–14</sup>, CNTs, have received significant attention. These compounds benefit from some excellent properties, such as inertness, high surface area, thermal and chemical stability, electric conductivity and tune-ability. These features attracted many scientists to utilize CNTs in various research fields, such as catalysis. One of the drawbacks of CNTs for the catalysis is their low wet-ability. This characteristic restricted the use of CNTs for the reactions in the aqueous media<sup>15–18</sup>. To furnish a solution to this issue, CNT can be functionalized or hybridized with hydrophilic moieties<sup>19</sup>.

Reduction of nitro functionality to amino group is a key chemical transformation that can be extensively utilized for the synthesis of complex chemicals and drugs<sup>20–22</sup>. Moreover, this reduction reaction can be exploited for de-colorization of dyes and waste water treatment. This catalytic process proceeds in the presence of conventional hydrogenation catalysts, such as Pd nanoparticles. To reduce the required content of the precious metals and

<sup>1</sup>Gas Conversion Department, Faculty of Petrochemicals, Iran Polymer and Petrochemical Institute, PO Box 14975-112, Tehran, Iran. <sup>2</sup>Department of Chemistry, School of Physics and Chemistry, Alzahra University, PO Box 1993891176, Vanak, Tehran, Iran. ✉email: s.sadjadi@ippi.ac.ir; mmheravi@alzahra.ac.ir

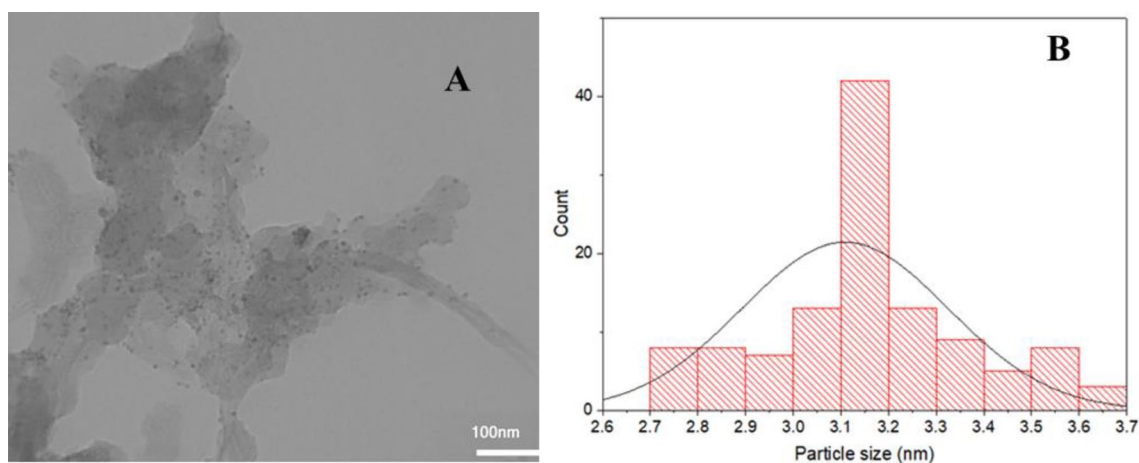


**Figure 1.** Schematic procedure for the preparation of Pd/CNT-P.

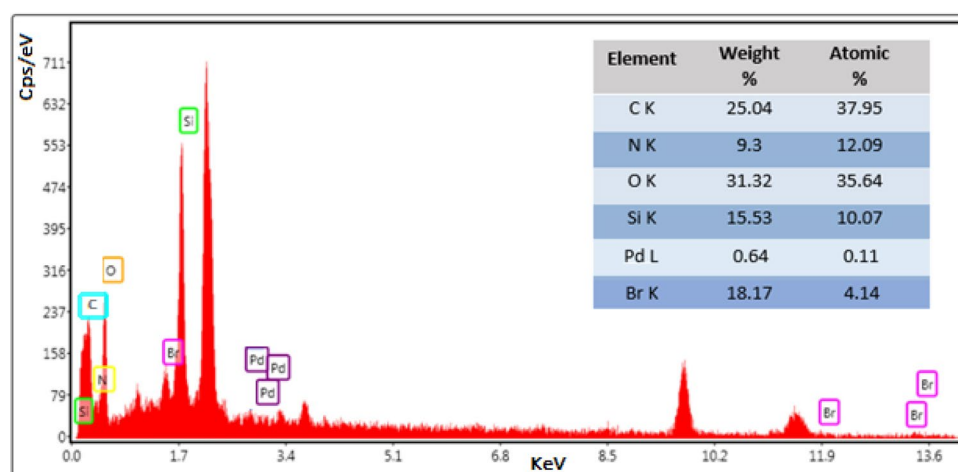
achieving fine nanoparticle size and high dispersion, supporting materials, such as clays<sup>24</sup> and carbohydrates<sup>25</sup> are employed.

Mostly, supporting materials are modified by introduction of functional groups on their surface. This can be conducted through covalent or non-covalent approaches<sup>26</sup>. In this regard, one of the most investigated functional groups is ionic liquid, IL<sup>27–29</sup> that is an organic salt with low toxicity<sup>27,30,31</sup>. As ILs are electrically charged species, they can be a promising compounds to provide electrostatic interactions with metallic nanoparticles and stabilizing them on the support. On the other hand, these compounds can also exhibit catalytic activity<sup>32,33</sup>. To date various IL-based catalysts have been developed for various chemical transformations<sup>34–39</sup>.

In the pursuit of our research on the heterogeneous catalysts<sup>24,40–45</sup>, in this project we wish to report a novel heterogeneous catalyst, Pd/CNT-P, with utility for hydrogenation of nitro compounds under mild reaction condition. To prepare the catalyst, silica-coated CNT has been synthesized and then vinyl functionalized. The resulted compound was then polymerized with the as-prepared 1-vinyl-3-butylimidazolium bromide (VBIB) and *N*-isopropylacrylamide (NIPAM) to furnish a thermo-responsive composite, which was subsequently palladated to give the hydrogenation catalyst (Fig. 1).



**Figure 2.** (A) TEM image of Pd/CNT-P and (B) particle size distribution of Pd nanoparticles.



**Figure 3.** EDS analysis of Pd/CNT-P.

## Result and discussion

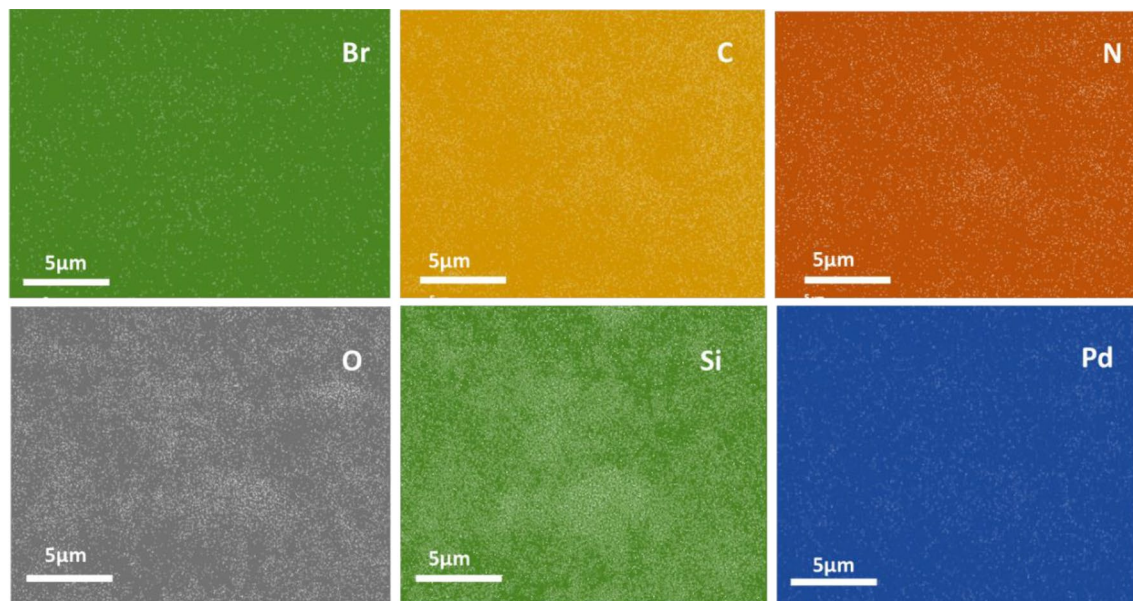
**Structure of the catalyst.** To study the morphology of Pd/CNT-P, it was analyzed via TEM. In TEM image of Pd/CNT-P (Fig. 2), polymeric moiety on the CNT tubes can be discerned. On the other hand, fine Pd nanoparticles (average diameter of  $4.0 \pm 0.1$  nm) can be seen on the CNT-P.

Pd/CNT-P was also characterized via EDS and elemental mapping analyses. As depicted in Fig. 3, the as-prepared catalyst contains C, N, O, Si, Pd and Br atoms. C, O and Si atoms can represent CNT-SiO<sub>2</sub>, while C, N, O and Br can be assigned to the P component. The presence of Pd also can indicate stabilization of Pd nanoparticles on CNT-P.

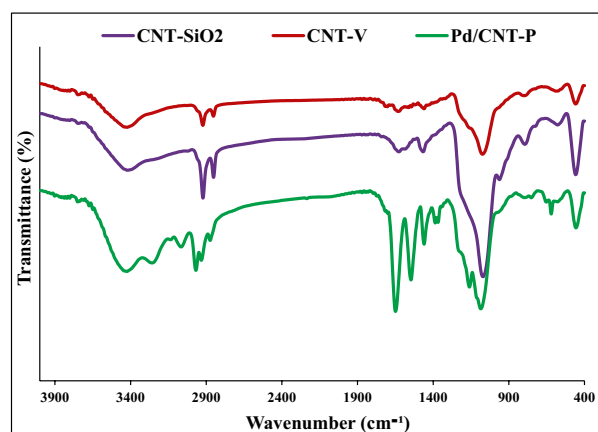
Elemental mapping analysis of Pd/CNT-P, Fig. 4, showed uniform dispersion of Pd, N and Br atoms. This observation implies that both polymeric component (P) and Pd nanoparticles have been distributed of CNT-SiO<sub>2</sub> homogeneously.

To confirm successful formation of CNT-SiO<sub>2</sub>, CNT-V and Pd/CNT-P, their FTIR spectrum has been recorded. As shown in Fig. 5, CNT-SiO<sub>2</sub> showed the absorbance bands at 1085 cm<sup>-1</sup> (Si-O-Si), 3410 cm<sup>-1</sup> (-OH), 1463 cm<sup>-1</sup> (-C-O), 2920 and 2850 cm<sup>-1</sup> (-CH<sub>2</sub> stretching). Moreover, the band at 1631 cm<sup>-1</sup> can be related to the -COOH functionality of the used CNT. CNT-V FTIR spectrum also exhibited the characteristic bands of CNT-SiO<sub>2</sub>, affirming the stability of CNT-SiO<sub>2</sub> upon functionalization. Moreover, the appearance of a small band at 1703 cm<sup>-1</sup> (-C=O) can confirm conjugation of TMSPPMA. In the FTIR spectrum of Pd/CNT-P, all of the characteristic absorbance bands of CNT-SiO<sub>2</sub> can be detected. Moreover, the appearance of sharp bands at 1645 cm<sup>-1</sup> (amidic -C=O) and 1546 cm<sup>-1</sup> (-C=N) can confirm conjugation of thermo-responsive co-polymer.

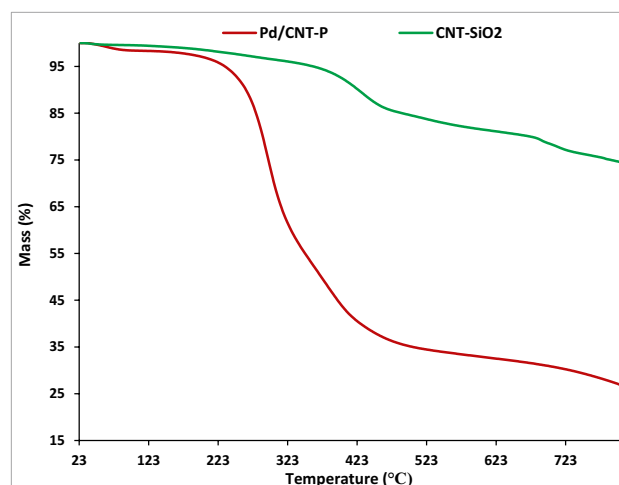
Thermogravimetric analysis of CNT-SiO<sub>2</sub> and Pd/CNT-P samples has been conducted to compare their thermal stability and confirm conjugation of P. As depicted in Fig. 6, CNT-SiO<sub>2</sub> showed high thermal stability. In fact, TG curve of CNT-SiO<sub>2</sub> showed two weight loss stages related to the loss of water (150 °C) and degradation of CNT (above 550 °C). TG curve of Pd/CNT-P is distinguished from TG curve of CNT-SiO<sub>2</sub>. In this curve an additional weight loss stage (44.3 wt.%) at 290 °C can be detected. This weight loss is assigned to the degradation of P component.



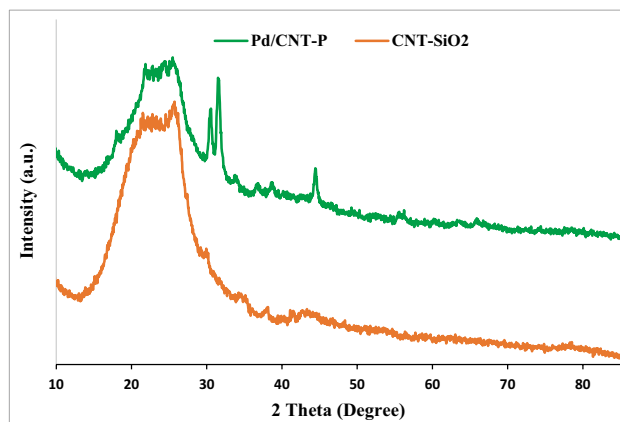
**Figure 4.** Elemental mapping of Pd/CNT-P.



**Figure 5.** FTIR spectra of CNT-SiO<sub>2</sub>, CNT-V and Pd/CNT-P.



**Figure 6.** TG curves of CNT-SiO<sub>2</sub> and Pd/CNT-P.



**Figure 7.** XRD patterns of Pd/CNT-P and CNT-SiO<sub>2</sub>.

Entry	Pd/CNT-P (mg)	Solvent	Temp. (°C)	Yield (%)
1	5	H <sub>2</sub> O	25	60 ± 2
2	5	EtOH	25	70 ± 2
3	5	CH <sub>3</sub> CN	25	70 ± 1
4	5	THF	25	70 ± 3
5	5	H <sub>2</sub> O:EtOH (1:1)	25	70 ± 3
6	10	H <sub>2</sub> O:EtOH (1:1)	25	80 ± 2
7	15	H <sub>2</sub> O:EtOH (1:1)	25	80 ± 2
8	10	H <sub>2</sub> O:EtOH (1:1)	30	85 ± 3
9	10	H <sub>2</sub> O:EtOH (1:1)	40	98 ± 3

**Table 1.** Optimization of the reaction condition for the model reaction.

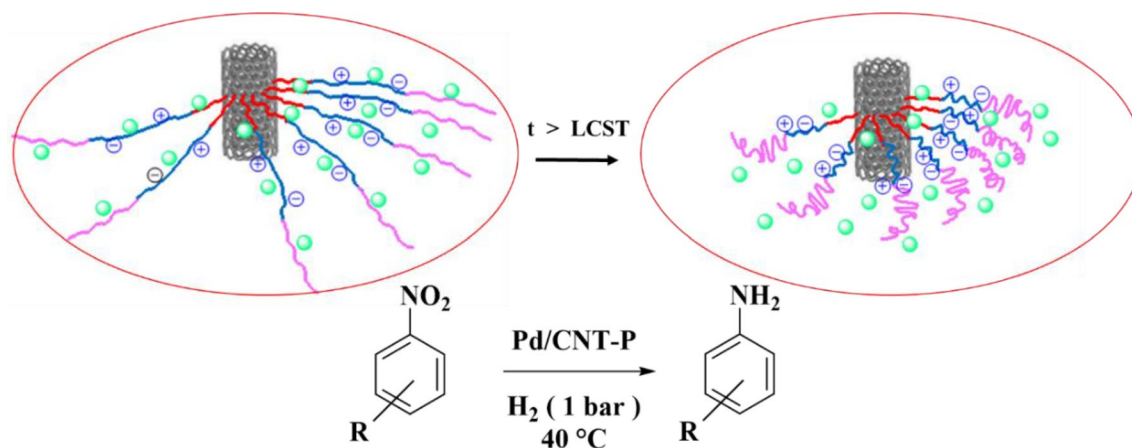
Using XRD analysis, the structure of Pd/CNT-P was investigated. In this regard, the XRD pattern of Pd/CNT-P was recorded and compared with that of CNT-SiO<sub>2</sub> (Fig. 7). The broad peak in the XRD pattern of CNT-SiO<sub>2</sub> can be assigned to the amorphous silica coat and approve successful coverage of CNT with SiO<sub>2</sub>. Other small peaks can be attributed to CNT. In the XRD pattern of Pd/CNT-P, the CNT-SiO<sub>2</sub> characteristic peaks can be detected. Noteworthy, the characteristic peak of the polymeric moiety ( $2\theta = 15\text{--}25^\circ$ ) overlapped with the characteristic peaks of CNT-SiO<sub>2</sub><sup>19</sup>. It is worth mentioning that the characteristic peaks of Pd nanoparticles were not discerned in the XRD pattern of Pd/CNT-P. This is assigned to the low content and high dispersion of Pd nanoparticles<sup>46</sup>.

**Activity of the catalyst.** Hydrogenation of nitro compounds is an important chemical reaction. This reaction not only is used for the synthesis of anilines, but also is applied for the synthesis of key chemical intermediates that can potentially be utilized for the synthesis of complicated organic compounds and drugs. Considering the importance of this reaction, we examined the catalytic activity of Pd/CNT-P for the hydrogenation of nitro compounds. To initiate the experiments, hydrogenation of nitrobenzene was selected as a model hydrogenation reaction. In the first step, the optimum reaction condition was found by studying the effects of reaction solvent, temperature and Pd/CNT-P loading on the yield of aniline.

First, the effect of the reaction solvent was appraised. In this regard, hydrogenation of nitrobenzene at room temperature and 5 mg Pd/CNT-P was performed in H<sub>2</sub>O, EtOH, H<sub>2</sub>O:EtOH (1:1), CH<sub>3</sub>CN and THF. As tabulated in Table 1, the reaction in water led to slightly lower yield of aniline. In the other four solvents, similar yields of aniline were furnished, indicating that the nature of solvent did not have a significant effect on the yield of the reaction. Considering these results and environmental concerns, H<sub>2</sub>O:EtOH (1:1) was selected as the reaction solvent.

In the next step, the effect of Pd/CNT-P loading was examined by repeating the model reaction in the presence of 5, 10 and 15 mg of Pd/CNT-P loading. As summarized in Table 1, by increasing the loading of the catalyst to 10 mg, the reaction yield increased from 70 to 80%. However, more increment of Pd/CNT-P loading did not improve the reaction yield. Therefore, 10 mg Pd/CNT-P was selected as the best loading.

Finally, the effect of the reaction temperature was investigated. To this purpose, the model reaction was conducted at 25, 30 and 40 °C. According to the results, elevating the reaction temperature was beneficiary for the reaction yield and the increase of the reaction temperature above LCST resulted in higher yield of aniline. This observation is in good accordance to the previous reports<sup>10,47</sup>. In fact, at temperature above the LCST (~37 °C),



**Figure 8.** Schematic presentation of structural change of the thermo-responsive catalyst at temperature above LCST for the hydrogenation of nitro compounds.

P component in the backbone of Pd/CNT-P collapses to furnish a hydrophobic periphery that is favorable for the mass-transfer of hydrophobic reactants, Fig. 8.

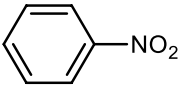
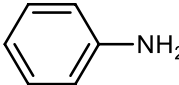

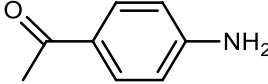
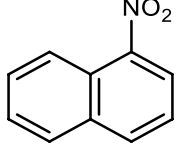
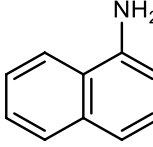
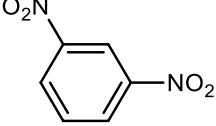
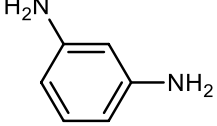
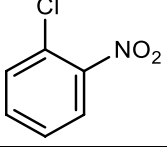
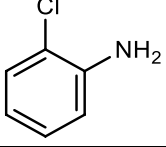
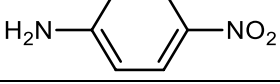

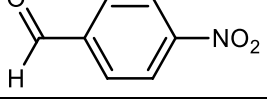
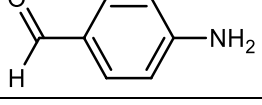
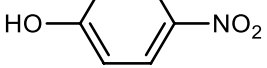
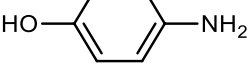
Having the optimum reaction condition in hand, other nitro compounds have been examined as substrates to confirm the generality of this protocol. As listed in Table 2, various nitro compounds can tolerate hydrogenation reaction under Pd/CNT-P catalysis to give the corresponding products in high yields. According to the results, the electronic feature of the substrates did not significantly affect the yield of the expected products and the substrates with both electron-donating and electron-withdrawing groups can furnish the products in high yields. However, steric effects can influence the reaction yield and huge and hydrophobic substrates led to lower yields. It is worth mentioning that Pd/CNT-P could catalyze the reaction of nitro compounds with carbonyl groups (4-nitroacetophenone and 4-nitrobenzaldehyde) selectively to give 4-aminoacetophenone and 4-aminobenzaldehyde as sole products. This observation approved high selectivity of Pd/CNT-P towards reduction of nitro functionality.

**Control catalysts.** In this project, we aimed to design a thermos-responsive catalyst, which could promote hydrogenation of nitro-compounds in aqueous media efficiently. To this purpose, we conjugated P that is an IL-containing thermoresponsive polymer with CNT covalently to benefit from the characteristics of the two components and the possible synergism between them. To elucidate whether the activity of the as-prepared composite is superior to each components, several control catalysts, including, Pd/PNIPAM Pd/P, Pd/CNT-V-PNIPAM, Pd/CNT-V, were prepared (Figure S1) and their activity for the model reaction was compared with that of Pd/CNT-P, Table 3. First, Pd/CNT-V was synthesized through the exact procedure used for the palladation of CNT-P, except, CNT-V was applied as a support and its activity was evaluated for the model reaction under the optimum reaction condition. As shown in Table 3, Pd/CNT-V showed moderate activity and led to the formation of aniline in 45% yield. Moreover, this sample was not thermos-responsive and its recovery from the reaction media was tedious. This observation confirmed the necessity of the presence of P for achieving high catalytic performance.

Next, Pd/CNT-V-PNIPAM was prepared through polymerization of CNT-V and NIPAM, followed by palladation. The study of the catalytic activity of this sample that did not contain IL in its structure approved that its catalytic activity was lower than that of the catalyst. This result confirmed the importance of IL in the structure of the catalyst for achieving high activity.

Two other catalysts, Pd/PNIPAM and Pd/P were also prepared through palladation of PNIPAM and P. The catalytic studies showed that these two control samples that did not contain CNT exhibited moderate activity and led to the formation of aniline in 30 and 40% respectively. This observation affirmed the role of CNT in the catalysis. In conclusion, the higher activity of Pd/CNT-P compared to the studied control catalysts indicated the positive role of hybridization of P and CNT and the presence of IL in the catalytic activity. To appraise the origin of different catalytic activity of the control catalysts, they have been characterized via ICP. As shown in Table 3, the loadings of Pd in the control catalysts are different. In fact, it can be observed that the nature of the support can affect the capability of Pd loading. As this feature is an important factor on the catalytic activity of the catalyst, the control samples exhibited different activity. As tabulated, Pd/CNT-P possessed the highest Pd loading and showed the best catalytic activity. In Pd/CNT-V-PNIPAM, in which both CNT and polymeric moiety are present, the loading of Pd is also high and slightly lower than that of Pd/CNT-P. Hence, high catalytic activity was observed. In the case of other control catalysts, the Pd loadings were lower and moderate activity was detected.

**Recyclability.** As facile recovery and efficient recyclability are important factors for heterogeneous catalysts, recyclability of Pd/CNT-P for the model reaction was appraised. The recycling test was simply conducted by separation of Pd/CNT-P from the first run of the model reaction and its recovery through washing with toluene and drying at 50 °C in oven. The recovered Pd/CNT-P was then used as a catalyst for catalyzing the second run of the model reaction under similar condition. Upon completion of the reaction, the recovery-reuse cycle was

Entry	Substrate	Product	Time (min)	Yield (%)
1			60	98±2
2			80	95±1
3			120	80±3
4			120	95±2
5			120	90±2
6			120	95±3
7			120	90±1
8			120	98±2

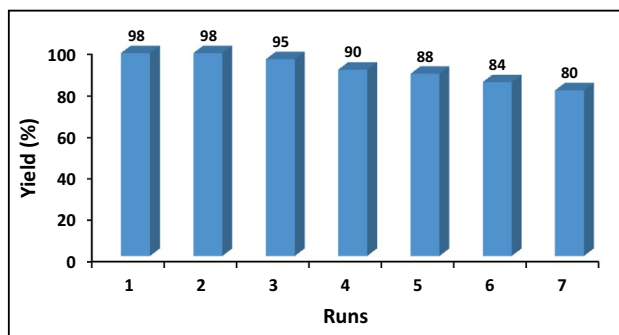
**Table 2.** Hydrogenation of nitro compounds under Pd/CNT-P catalysis<sup>a</sup>. <sup>a</sup>1 mmol nitro compound, H<sub>2</sub>O/EtOH (1/1), 40 °C under H<sub>2</sub> gas (1 bar).

Entry	Catalyst	Yield (%) <sup>a</sup>	Pd loading (wt.%)
1	Pd/PNIPAM	30	0.81
2	Pd/P	40	0.89
3	Pd/CNT-V-PNIPAM <sup>b</sup>	80	0.91
4	Pd/CNT-V	45	0.89
5	Pd/CNT-P	98	1

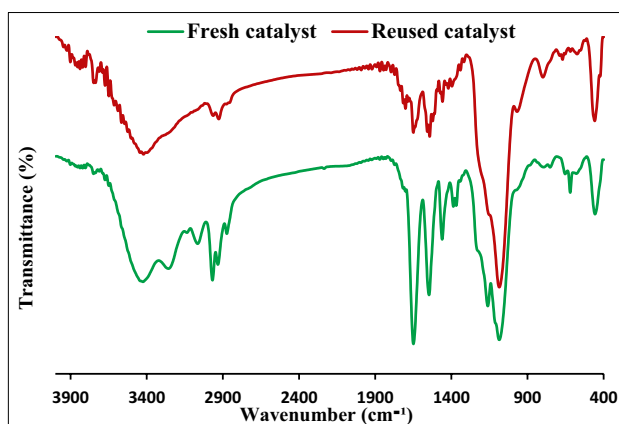
**Table 3.** Comparison of the catalytic activity of Pd/CNT-P and control catalysts for the nitrobenzene hydrogenation. <sup>a</sup>Reaction condition: nitrobenzene (1 mmol), catalyst (10 mg), H<sub>2</sub>O:EtOH (1:1), H<sub>2</sub> (1 bar) at 40 °C in 2 h. <sup>b</sup>Pd was loaded on the CNT-V, which was polymerized with NIPAM.

repeated for seven consecutive runs. As shown in Fig. 9, Pd/CNT-P can be efficiently recycled and only slight loss of the activity was detected after each recycling.

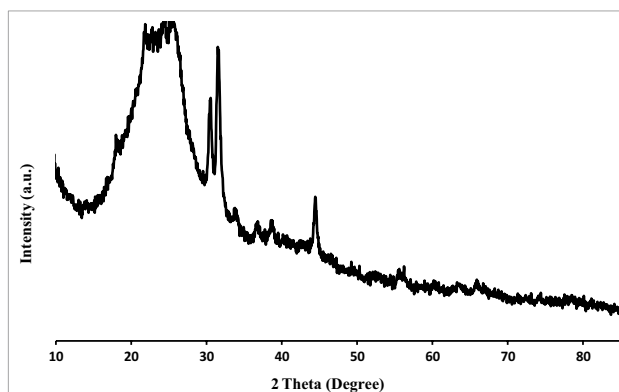
To study the stability of Pd/CNT-P structure upon recycling, the reused catalyst (obtained after seventh run) was characterized via FTIR spectroscopy. As shown in Fig. 10, the FTIR spectrum of the reused Pd/CNT-P exhibited all of the absorbance bands of fresh Pd/CNT-P. This observation affirms the stability of Pd/CNT-P upon recycling.



**Figure 9.** Recyclability of the catalyst for the model reaction under the optimum reaction condition.



**Figure 10.** Comparison of the FTIR spectra of fresh and recycled catalyst after seven runs.



**Figure 11.** XRD analysis of the recycled catalyst after seven runs.

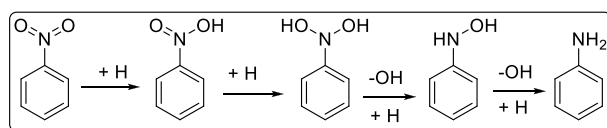
The measurement of leaching of Pd was performed via ICP analysis. To this purpose, the recovered catalyst after seventh run of the reaction was analyzed by ICP. It was found that Pd leaching was 1.6 wt.% of initial loading. According to these results and considering the fact that Pd species is the main component for promoting hydrogenation reaction, loss of the catalytic activity of the catalyst can be attributed to the Pd leaching.

To appraise the stability of Pd/CNT-P in the course of recyclability, the recovered Pd/CNT-P after seventh run of the hydrogenation reaction was analyzed via XRD. As presented in Fig. 11, the recorded XRD pattern of the recovered Pd/CNT-P is identical to that of fresh one, confirming the stability of the catalyst under recovering-cycles.



Entry	Catalyst	Solvent	H <sub>2</sub> Pressure	Time (min)	Temp. (°C)	Yield (%)	Refs.
1	PdNP(0.5%)/Al <sub>2</sub> O <sub>3</sub> (0.3 g)	THF	1 atm	180	r.t	100	48
2	Pd@Hal-Hydrogel + cyclodextrin (2 wt.%)	H <sub>2</sub> O	1 bar	120	50	95	49
3	Pd@Hal-TCT-Met <sup>a</sup>	H <sub>2</sub> O	1 bar	75	65	100	50
4	APSNP <sup>b</sup> (1 mol%)	EtOH	40 atm	120	r.t	100	51
5	Pd@CS-CD-MGQDs <sup>c</sup> (0.5 mol%)	H <sub>2</sub> O	1 atm	60	50	97	52
6	Pd/PPh <sub>3</sub> @FDU-12 (8.33 × 10 <sup>-4</sup> mmol Pd)	EtOH	10 bar	60	40	99	53
7	Pd@Hal-biochar <sup>d</sup> (0.03 mol%)	H <sub>2</sub> O	1 bar	60	r.t	75	54
8	Pd@Hal/di-urea <sup>e</sup> (1.5 wt.%)	H <sub>2</sub> O	1 atm	60	50	100	55
9	Pd@Per-P(0.03 g)	H <sub>2</sub> O:EtOH (1:1)	1 atm	90	45	98	56
10	Pd@Hal-CCD <sup>f</sup> (1 wt.%)	H <sub>2</sub> O	1 atm	90	r.t	100	57
11	Pd/CNT-P	H <sub>2</sub> O:EtOH (1:1)	1 bar	120	40	98	This work

**Table 4.** The comparison of the activity of Pd@Per-P for the model hydrogenation reaction. <sup>a</sup>Pd immobilization on the multi-amine functionalized halloysite. <sup>b</sup>Activated palladium sucrose nanoparticles. <sup>c</sup>Pd on hybrid of magnetic graphene dots and cyclodextrin decorated chitosan. <sup>d</sup>Hybrid of halloysite and char. <sup>e</sup>Halloysite clay decorated with ligand. <sup>f</sup>Halloysite decorated with cyclodextrin derived carbon sphere.



**Figure 12.** The proposed mechanism for the hydrogenation of nitrobenzene.

**Hot filtration test.** There are two possibilities in heterogeneous catalysis. In true heterogeneous catalysis, it is expected that the catalytic species remains stabilized on the support, while in the second possibility, the catalytic species can leach to the reaction media and then stabilized on the support. The well-known test for determining the nature of the catalysis is hot filtration, in which the catalyst is removed from the reaction after a short period and then the reaction is pursued in the absence of the catalyst. In the case of true heterogeneous catalysis, in which no leaching of the catalytic species occurs, the reaction does not proceed after removal of the catalyst, while in the other pass way, the reaction proceeds in the absence of the catalyst due to the leached catalytic species. Hot filtration test approved that Pd/CNT-P was a true heterogeneous catalyst. In more detail, hydrogenation of nitrobenzene did not proceed after removing of Pd/CNT-P from the reaction vessel.

**Comparative study.** The activity of Pd/CNT-P for the hydrogenation of nitrobenzene was compared with some of the Pd-based catalysts, reported in the literature, Table 4. As illustrated, Pd nanoparticles have been supported on various supporting materials. Moreover, different reaction conditions have been reported using the tabulated catalysts. Although in some catalysts, available and low-cost supports, such as Al<sub>2</sub>O<sub>3</sub> and sucrose nanoparticles has been reported, high hydrogen pressure or toxic solvents were used for achieving high yield of aniline. In some reports, halloysite nanoclay has been utilized for the immobilization of Pd nanoparticles. Although halloysite is a natural clay, it is relatively costly. On the other hand, mostly, halloysite is modified chemically through multi-step procedures, using toxic reagents and solvents prior to Pd stabilization. This issue negatively affects the cost of the final catalyst. Metal organic frameworks have also been employed as a support. In this case, the required hydrogen pressure was high that is not favorable from environmental point of view. On the other hand, synthesis of metal organic frameworks is a delicate process, using some costly linkers.

**Reaction mechanism.** According to the previous reports, the possible mechanism for the hydrogenation of nitroarenes can be depicted as Fig. 12<sup>58</sup>. As illustrated, hydrogenation reaction proceeds via double H-induced dissociation of N–O bond, in which the Pd species on the CNT-P can play role in activation of the substrate.

## Experimental section

**Materials and instruments.** COOH-functionalized multi-wall carbon nanotubes (MWCNTs) (purity > 95%, content of COOH = 3.86 wt.%, inner diameter: 2–5 nm and outer diameter > 7 nm) were obtained from US Research Nanomaterials. Other reagents and solvents applied for the synthesis of the catalyst and conducting hydrogenation reaction of nitro-compounds are as follow: (3-trimethoxysilyl) propyl methacrylate (TMSPMA), cetyltrimethyl ammonium bromide (CTAB), tetraethyl orthosilicate (TEOS), 1-vinylimidazole, NIPAM, azobisisobutyronitrile (AIBN), triethylamine (Et<sub>3</sub>N), palladium(II) acetate Pd(OAc)<sub>2</sub>, sodium borohydride (NaBH<sub>4</sub>), *N,N*-dimethylformamide (DMF), nitro-compounds, 1-bromo butane, sodium hydroxide, tolu-

ene, ethanol (EtOH) and methanol (MeOH), all was purchased from Sigma-Aldrich (Germany, Taufkirchen) and used without further purification.

The formation of Pd/CNT-P was confirmed by various characterization techniques, including: Fourier transform Infrared spectroscopy (FT-IR), X-ray diffraction (XRD), thermogravimetric analysis (TGA), transmission electron microscopy (TEM), inductively coupled plasma mass spectroscopy (ICP-MS), energy-dispersive X-ray spectroscopy (EDS) and elemental mapping analysis.

Recording of FTIR spectra was carried out by using BRUKER TENSOR 35 spectrophotometer 65 with scan time of 1 s and spectral resolution of  $2\text{ cm}^{-1}$  by using KBr pellets. The XRD pattern of Pd/CNT-P was recorded using a Rigaku Ultima IV with Cu K $\alpha$  radiation from a sealed tube. Thermal stability of Pd/CNT-P was investigated by applying METTLER TOLEDO thermogravimetric analysis apparatus. To record the catalyst thermogram, inert atmosphere and heating rate of  $10\text{ }^\circ\text{C min}^{-1}$  were applied. TEM images of Pd/CNT-P were recorded on a Phillips EM 208S microscope at 100 kV. Pd loading of Pd/CNT-P was estimated using ICP analyzer Varian, Vista-pro instrument. EDX and elemental mapping analyses were carried out by Tescan Mira II.

## Preparation of Pd/CNT-P

**Surface modification of carbon nanotubes: synthesis of CNT-SiO<sub>2</sub>.** Surface modification of CNT with silica was performed according to the previous report<sup>59</sup>. Typically, to a solution of CTAB (1.7 g) in distilled water (40 ml), CNT (0.2 g) was added and the resulting suspension was homogenized under ultrasonic irradiation (160 W for 30 min). Afterwards, NaOH (0.08 g) was added and the resulting mixture was stirred for 30 min at 60 °C. In the next step, a solution of TEOS (10 mL) in EtOH was introduced to the aforementioned suspension under stirring condition at 60 °C. After 24 h, the product, CNT-SiO<sub>2</sub>, was separated via centrifugation, washed repeatedly with warm EtOH and dried in oven overnight.

**Vinyl-functionalization of CNT-SiO<sub>2</sub>: synthesis of CNT-V.** In order to vinyl-functionalize CNT-SiO<sub>2</sub>, the as-prepared CNT-SiO<sub>2</sub> (0.5 g) was dispersed in dry toluene (20 mL) by using ultrasonic irradiation (160 W) for 20 min. Then TMSPMA (0.5 g) was added to CNT-SiO<sub>2</sub> suspension and the resulting mixture was refluxed at 110 °C for 24 h under Ar atmosphere. Upon completion of the reaction, the precipitate, CNT-V, was collected via centrifuge, washed with toluene and dried in oven at 80 °C overnight.

**Synthesis of VBIB.** VBIB was prepared according to the previous report<sup>60</sup>. Briefly, the mixture of 1-bromobutane (4 g) and 1-vinylimidazole (2 g) was stirred at 70 °C under solvent-free condition for 16 h under inert atmosphere. Then, the reaction mixture was allowed to cool to room temperature and the product was collected, washed several times with ethyl acetate and dried in a vacuum oven overnight.

**Polymerization of NIPAM, VBIB and CNT-V: synthesis of CNT-P.** CNT-V (0.5 g) was added to a solution of NIPAM (0.5 g) in DMF (20 mL) under stirring condition under Ar atmosphere at 70 °C. After 20 min, a solution of AIBN (0.15 g) in DMF (10 mL) was added to the aforesaid mixture in a dropwise manner and stirring was maintained for 40 min. Subsequently, a solution of VBIB (0.5 g) in DMF (10 mL) was added and the resulting mixture was stirred for 24 h at 70 °C under Ar atmosphere. After completion of the reaction, the solvent was evaporated and the solid was collected, rinsed with DMF and dried in oven at 70 °C overnight.

**Immobilization of Pd nanoparticles on CNT-P: Synthesis of Pd/CNT-P.** In order to prepare Pd/CNT-P, CNT-P (1.5 g) was stirred in toluene (20 mL) in a 2-neck round flask under Ar atmosphere at room temperature for 30 min. Subsequently, a solution of Pd(OAc)<sub>2</sub> (0.02 g) in toluene (15 mL) was gently introduced to the aforementioned suspension. After 1 h, a solution of NaBH<sub>4</sub> (0.2 N) in MeOH (20 mL) was slowly added and the obtained mixture was stirred for 2 h. Finally, the as-prepared Pd/CNT-P was collected via centrifugation, washed with toluene and dried in oven at 50 °C overnight, Fig. 1. According to the ICP analysis, Pd loading in Pd/CNT-P was 1 wt.%.

**Typical procedure for the hydrogenation of nitro-compounds.** Hydrogenation of nitro-compounds was conducted under mild reaction condition. Typically, a mixture of nitro aromatic compound (1 mmol) and Pd/CNT-P (0.01 g) in H<sub>2</sub>O/EtOH (1/1) was heated to 40 °C under H<sub>2</sub> gas (1 bar). The progress of the hydrogenation reaction was traced by TLC. Upon completion of the process, Pd/CNT-P was separated and recovered by washing with toluene (30 mL) and drying at 50 °C in an oven overnight. The recovered catalyst was reused for the next run of the reaction. The hydrogenized product was obtained after evaporation of the solvent. The reaction yield was measured via GC analysis.

## Conclusion

A novel thermo-responsive catalyst, Pd/CNT-P, was designed and synthesized through vinyl functionalization of CNT-SiO<sub>2</sub>, followed by polymerization with NIPAM and VBIB and palladation. The catalytic performance of the resulting catalyst was examined for the hydrogenation of nitro-compounds in aqueous media under mild reaction condition. The results affirmed high catalytic activity of the catalyst, broad substrate scope and high selectivity of the catalyst towards nitro group. Moreover, the catalyst was recyclable up to seven reaction runs with slight Pd leaching. Hot filtration test also indicated the true heterogeneous nature of the catalysis. The comparison of the catalytic activity of Pd/CNT-P with several control catalysts confirmed the importance of conjugation of P and CNT for achieving high catalytic activity.

Received: 7 December 2021; Accepted: 16 February 2022

Published online: 10 March 2022

## References

- Ahn, Y., Jang, Y., Selvapalam, N., Yun, G. & Kim, K. Supramolecular velcro for reversible underwater adhesion. *Angew. Chem. Int. Ed.* **52**, 3140–3144 (2013).
- Guo, J., Yuan, C., Guo, M., Wang, L. & Yan, F. Flexible and voltage-switchable polymer velcro constructed using host–guest recognition between poly (ionic liquid) strips. *Chem. Sci.* **5**, 3261–3266 (2014).
- Chen, F., Ren, Y., Guo, J. & Yan, F. Thermo- and electro-dual responsive poly (ionic liquid) electrolyte based smart windows. *Chem. Commun.* **53**, 1595–1598 (2017).
- Jiang, H., Kelch, S. & Lendlein, A. Polymers move in response to light. *Adv. Mater.* **18**, 1471–1475 (2006).
- Li, J. *et al.* Enhanced photocatalytic activity of g-C<sub>3</sub>N<sub>4</sub>-ZnO/HNTs composite heterostructure photocatalysts for degradation of tetracycline under visible light irradiation. *RSC Adv.* **5**, 91177–91189. <https://doi.org/10.1039/C5RA17360D> (2015).
- Roy, D., Brooks, W. L. & Sumerlin, B. S. New directions in thermoresponsive polymers. *Chem. Soc. Rev.* **42**, 7214–7243 (2013).
- Xiao, Y.-Y. *et al.* Light-, pH- and thermal-responsive hydrogels with the triple-shape memory effect. *Chem. Commun.* **52**, 10609–10612 (2016).
- Moon, H. C., Lodge, T. P. & Frisbie, C. D. Solution processable, electrochromic ion gels for sub-1 V, flexible displays on plastic. *Chem. Mater.* **27**, 1420–1425 (2015).
- Beaujuge, P. M. & Reynolds, J. R. Color control in  $\pi$ -conjugated organic polymers for use in electrochromic devices. *Chem. Rev.* **110**, 268–320 (2010).
- Massaro, M. *et al.* Design of PNIPAAm covalently grafted on halloysite nanotubes as a support for metal-based catalysts. *RSC Adv.* **6**, 55312–55318 (2016).
- Shibayama, M., Suetoh, Y. & Nomura, S. Structure relaxation of hydrophobically aggregated poly (N-isopropylacrylamide) in water. *Macromolecules* **29**, 6966–6968 (1996).
- Stodolak-Zych, E. *et al.* Spectroscopic studies of the influence of CNTs on the thermal conversion of PAN fibrous membranes to carbon nanofibers. *J. Mol. Struct.* **1126**, 94–102. <https://doi.org/10.1016/j.molstruc.2016.01.022> (2016).
- Sheikhi, M. *et al.* Adsorption properties of the molecule resveratrol on CNT(8,0–10) nanotube: Geometry optimization, molecular structure, spectroscopic (NMR, UV/Vis, excited state), FMO, MEP and HOMO-LUMO investigations. *J. Mol. Struct.* **1160**, 479–487. <https://doi.org/10.1016/j.molstruc.2018.01.005> (2018).
- Khosroshahy, M. B., Daliri, M. S., Abdoli, A., Navi, K. & Bagherzadeh, N. A 3D universal structure based on molecular-QCA and CNT technologies. *J. Mol. Struct.* **1119**, 86–95. <https://doi.org/10.1016/j.molstruc.2016.04.025> (2016).
- Fan, J.-J. *et al.* A novel strategy for sulfur-doped carbon nanotube as a high efficient Pt catalyst support toward methanol oxidation reaction. *J. Mater. Chem. A* **5**, 19467–19475 (2017).
- Hiltrop, D. *et al.* Pd deposited on functionalized carbon nanotubes for the electrooxidation of ethanol in alkaline media. *Electrochem Commun.* **63**, 30–33 (2016).
- Ombaka, L. M., Ndungu, P. & Nyamori, V. O. Usage of carbon nanotubes as platinum and nickel catalyst support in dehydrogenation reactions. *Catal. Today* **217**, 65–75 (2013).
- Wang, W., Chu, W., Wang, N., Yang, W. & Jiang, C. Mesoporous nickel catalyst supported on multi-walled carbon nanotubes for carbon dioxide methanation. *Int. J. Hydrogen Energy* **41**, 967–975 (2016).
- Sadjadi, S., Heravi, M. M. & Raja, M. Combination of carbon nanotube and cyclodextrin nanosponge chemistry to develop a heterogeneous Pd-based catalyst for ligand and copper free C-C coupling reactions. *Carbohydr. Polym.* **185**, 48–55. <https://doi.org/10.1016/j.carbpol.2018.01.020> (2018).
- Metin, Ö., Can, H., Şendil, K. & Gültekin, M. S. Monodisperse Ag/Pd core/shell nanoparticles assembled on reduced graphene oxide as highly efficient catalysts for the transfer hydrogenation of nitroarenes. *J. Colloid Interface Sci.* **498**, 378–386 (2017).
- Parida, K., Varadwaj, G. B. B., Sahu, S. & Sahoo, P. C. Schiff base Pt (II) complex intercalated montmorillonite: A robust catalyst for hydrogenation of aromatic nitro compounds at room temperature. *Ind. Eng. Chem. Res.* **50**, 7849–7856 (2011).
- Song, J. *et al.* Review on selective hydrogenation of nitroarene by catalytic, photocatalytic and electrocatalytic reactions. *Appl. Catal. B* **227**, 386–408 (2018).
- Vahedi-Notash, N., Heravi, M. M., Alhampour, A. & Mohammadi, P. Ag nanoparticles immobilized on new mesoporous triazine-based carbon (MTC) as green and recoverable catalyst for reduction of nitroaromatic in aqueous media. *Sci. Rep.* **10**, 19322. <https://doi.org/10.1038/s41598-020-74232-4> (2020).
- Sadjadi, S. Halloysite-based hybrids/composites in catalysis. *Appl. Clay Sci.* **189**, 105537. <https://doi.org/10.1016/j.clay.2020.105537> (2020).
- Leonhardt, S. E. S. *et al.* Chitosan as a support for heterogeneous Pd catalysts in liquid phase catalysis. *Appl. Catal. A-Gen.* **379**, 30–37. <https://doi.org/10.1016/j.apcata.2010.02.029> (2010).
- Sadjadi, S. Magnetic (poly) ionic liquids: A promising platform for green chemistry. *J. Mol. Liq.* **323**, 114994. <https://doi.org/10.1016/j.molliq.2020.114994> (2021).
- Karimi, F., Zolfigol, M. A. & Yarie, M. A novel and reusable ionically tagged nanomagnetic catalyst: Application for the preparation of 2-amino-6-(2-oxo-2H-chromen-3-yl)-4-arylnicotinonitriles via vinyllogous anionic based oxidation. *Mol. Catal.* **463**, 20–29. <https://doi.org/10.1016/j.mcat.2018.11.009> (2019).
- Sadjadi, S., Akbari, M. & Heravi, M. M. Palladated nanocomposite of halloysite–nitrogen-doped porous carbon prepared from a novel cyano-/nitrile-free task specific ionic liquid: An efficient catalyst for hydrogenation. *ACS Omega* **4**, 19442–19451. <https://doi.org/10.1021/acsomega.9b02887> (2019).
- Öztürk, B. Ö. Ammonium tagged Hoveyda-Grubbs catalysts immobilized on magnetically separable core-shell silica supports for ring-closing metathesis reactions. *Microporous Mesoporous Mater.* **267**, 249–256. <https://doi.org/10.1016/j.micromeso.2018.04.002> (2018).
- Teimuri-Mofrad, R., Gholamhosseini-Nazari, M., Payami, E. & Esmati, S. Ferrocene-tagged ionic liquid stabilized on silica-coated magnetic nanoparticles: Efficient catalyst for the synthesis of 2-amino-3-cyano-4H-pyran derivatives under solvent-free conditions. *Appl. Organomet. Chem.* **32**, e3955. <https://doi.org/10.1002/aoc.3955> (2018).
- Rafee, E. & Kahrizi, M. Mechanistic investigation of Heck reaction catalyzed by new catalytic system composed of Fe<sub>3</sub>O<sub>4</sub>@OA–Pd and ionic liquids as co-catalyst. *J. Mol. Liq.* **218**, 625–631. <https://doi.org/10.1016/j.molliq.2016.02.055> (2016).
- Feng, H., He, C., Ma, G. & Zhiani, R. Imidazolium ionic liquid functionalized nano dendritic CuAl<sub>2</sub>O<sub>4</sub> for visible light-driven photocatalytic degradation of dye pollutant. *Inorg. Chem. Commun.* **132**, 108818. <https://doi.org/10.1016/j.inoche.2021.108818> (2021).
- Afzali, E., Mirjafari, Z., Akbarzadeh, A. & Saeidian, H. vComplexation of copper ion-containing immobilized ionic liquid in designed hierarchical-functionalized layered double hydroxide nanoreactor for azide–alkyne cycloaddition reaction. *Inorg. Chem. Commun.* **132**, 108858. <https://doi.org/10.1016/j.inoche.2021.108858> (2021).
- Tan, J., Rui Li, J. & Lin Hu, Y. Novel and efficient multifunctional periodic mesoporous organosilica supported benzotriazolium ionic liquids for reusable synthesis of 2,4,5-trisubstituted imidazoles. *J. Saudi Chem. Soc.* **24**, 777–784. <https://doi.org/10.1016/j.jscs.2020.08.006> (2020).

35. Yao, N., Lu, M., Liu, X. B., Tan, J. & Hu, Y. L. Copper-doped mesoporous silica supported dual acidic ionic liquid as an efficient and cooperative reusability catalyst for Biginelli reaction. *J. Mol. Liq.* **262**, 328–335. <https://doi.org/10.1016/j.molliq.2018.04.121> (2018).
36. Rui Li, J., Chen, C. & Lin Hu, Y. Novel and efficient Knoevenagel condensation over mesoporous SBA-15 supported acetate-functionalized basic ionic liquid catalyst. *ChemistrySelect* **5**, 14578–14582. <https://doi.org/10.1002/slct.202004048> (2020).
37. Jin, T., Dong, F., Liu, Y. & Hu, Y. L. Novel and effective strategy of dual bis(trifluoromethylsulfonyl)imide imidazolium ionic liquid immobilized on periodic mesoporous organosilica for greener cycloaddition of carbon dioxide to epoxides. *New J. Chem.* **43**, 2583–2590. <https://doi.org/10.1039/C8NJ05273E> (2019).
38. Hu, Y. L., Zhang, R. L. & Fang, D. Quaternary phosphonium cationic ionic liquid/porous metal–organic framework as an efficient catalytic system for cycloaddition of carbon dioxide into cyclic carbonates. *Environ. Chem. Lett.* **17**, 501–508. <https://doi.org/10.1007/s10311-018-0793-9> (2019).
39. Yao, N., Chen, C., Li, D. J. & Hu, Y. L. Cobalt nanoparticles embedded over periodic mesoporous organosilica functionalized with benzotriazolium ionic liquid for efficient and heterogeneous catalytic transformation of carbon dioxide to cyclic carbonates. *J. Environ. Chem. Eng.* **8**, 103953. <https://doi.org/10.1016/j.jece.2020.103953> (2020).
40. Tabrizi, M. *et al.* Efficient hydro-finishing of polyalphaolefin based lubricants under mild reaction condition using Pd on ligands decorated halloysite. *J. Colloid Interface Sci.* **581**, 939–953. <https://doi.org/10.1016/j.jcis.2020.08.112> (2021).
41. Sadjadi, S., Lazzara, G., Malmir, M. & Heravi, M. M. Pd nanoparticles immobilized on the poly-dopamine decorated halloysite nanotubes hybridized with N-doped porous carbon monolayer: A versatile catalyst for promoting Pd catalyzed reactions. *J. Catal.* **366**, 245–257. <https://doi.org/10.1016/j.jcat.2018.08.013> (2018).
42. Sadjadi, S., Akbari, M., Léger, B., Monflier, E. & Heravi, M. M. Eggplant-derived biochar-halloysite nanocomposite as supports of Pd nanoparticles for the catalytic hydrogenation of nitroarenes in the presence of cyclodextrin. *ACS Sustain. Chem. Eng.* **7**, 6720–6731. <https://doi.org/10.1021/acssuschemeng.8b05992> (2019).
43. Karimi, S. *et al.* Pd on nitrogen rich polymer–halloysite nanocomposite as an environmentally benign and sustainable catalyst for hydrogenation of polyalphaolefin based lubricants. *J. Ind. Eng. Chem.* **97**, 441–451. <https://doi.org/10.1016/j.jiec.2021.02.031> (2021).
44. Sadjadi, S., Koohestani, F. & Heravi, M. M. Fabrication of a metal free catalyst for chemical reactions through decoration of chitosan with ionic liquid terminated dendritic moiety. *Sci. Rep.* **10**, 19666. <https://doi.org/10.1038/s41598-020-76795-8> (2020).
45. Sadjadi, S., Malmir, M., Lazzara, G., Cavallaro, G. & Heravi, M. M. Preparation of palladated porous nitrogen-doped carbon using halloysite as porogen: Disclosing its utility as a hydrogenation catalyst. *Sci. Rep.* **10**, 2039. <https://doi.org/10.1038/s41598-020-59003-5> (2020).
46. Mallik, S., Dash, S. S., Parida, K. M. & Mohapatra, B. K. Synthesis, characterization, and catalytic activity of phosphomolybdic acid supported on hydrous zirconia. *J. Colloid Interface Sci.* **300**, 237–243 (2006).
47. Gao, C., Möhwald, H. & Shen, J. Thermosensitive poly (allylamine)-g-poly (N-isopropylacrylamide): Synthesis, phase separation and particle formation. *Polymer* **46**, 4088–4097 (2005).
48. Agrahari, S., Lande, S., Balachandran, V., Kalpana, G. & Jasra, R. Palladium Supported on Mesoporous Alumina Catalyst for Selective Hydrogenation. *J. Nanosci. Curr. Sci.* **2**, 1000114. <https://doi.org/10.4172/2572-0813.1000114> (2017).
49. Sadjadi, S. & Atai, M. Palladated halloysite hybridized with photo-polymerized hydrogel in the presence of cyclodextrin: An efficient catalytic system benefiting from nanoreactor concept. *Appl. Organomet. Chem.* **33**, e4776. <https://doi.org/10.1002/aoc.4776> (2019).
50. Sadjadi, S., Koohestani, F. & Bahri-Laleh, N. Pd immobilization on the multi-amine functionalized halloysite as an efficient catalyst for hydrogenation reaction: An experimental and computational study. *Appl. Clay Sci.* **192**, 105645. <https://doi.org/10.1016/j.clay.2020.105645> (2020).
51. Samsonu, D., Brahmaya, M., Govindh, B. & Murthy, Y. Green synthesis & catalytic study of sucrose stabilized Pd nanoparticles in reduction of nitro compounds to useful amines. *S. Afr. J. Chem. Eng.* **25**, 110–115 (2018).
52. Esmailzadeh, M., Sadjadi, S. & Salehi, Z. Pd immobilized on hybrid of magnetic graphene quantum dots and cyclodextrin decorated chitosan: An efficient hydrogenation catalyst. *Int. J. Biol. Macromol.* **150**, 441–448. <https://doi.org/10.1016/j.ijbiomac.2020.02.094> (2020).
53. Guo, M. *et al.* Improving catalytic hydrogenation performance of Pd nanoparticles by electronic modulation using phosphine ligands. *ACS Catal.* **8**, 6476–6485 (2018).
54. Sadjadi, S., Akbari, M., Leger, B., Monflier, E. & Heravi, M. Eggplant-derived biochar-halloysite nanocomposite as supports of Pd nanoparticles for the catalytic hydrogenation of nitroarenes in presence of cyclodextrin. *ACS Sus. Chem. Eng.* **7**, 6720–6731 (2019).
55. Dehghani, S., Sadjadi, S., Bahri-Laleh, N., Nekoomanesh-Haghighi, M. Poater, A. Study of the effect of the ligand structure on the catalytic activity of Pd@ ligand decorated halloysite: Combination of experimental and computational studies. *Appl. Organomet. Chem.* **33**, e4891. <https://doi.org/10.1002/aoc.4891> (2019).
56. Abedian-Dehghani, N., Heravi, M. & Sadjadi, S. Pd on the Composite of Perlite and Allylamine-N-isopropylacrylamide Copolymer: A Thermo-Responsive Catalyst for Hydrogenation of Nitroarenes under Mild Reaction Condition. *Catalysts*. **11**, 1334. <https://doi.org/10.3390/catal11111334> (2021).
57. Sadjadi, S., Ghoreyshi Kahangi, F. & Heravi, M. M. Pd stabilized on nanocomposite of halloysite and  $\beta$ -cyclodextrin derived carbon: An efficient catalyst for hydrogenation of nitroarene. *Polyhedron* **175**, 114210. <https://doi.org/10.1016/j.poly.2019.114210> (2020).
58. Sheng, T. *et al.* Insights into the mechanism of nitrobenzene reduction to aniline over Pt catalyst and the significance of the adsorption of phenyl group on kinetics. *Chem. Eng. Sci.* **293**, 337–344. <https://doi.org/10.1016/j.ces.2016.02.066> (2016).
59. Sadjadi, S. & Koohestani, F. Pd immobilized on polymeric network containing imidazolium salt, cyclodextrin and carbon nanotubes: Efficient and recyclable catalyst for the hydrogenation of nitroarenes in aqueous media. *J. Mol. Liq.* **301**, 112414. <https://doi.org/10.1016/j.molliq.2019.112414> (2020).
60. Sadjadi, S., Koohestani, F. & Heravi, M. Biochar-Based Graphitic carbon nitride adorned with ionic liquid containing acidic polymer: A versatile, non-metallic catalyst for acid catalyzed reaction. *Molecules* **25**, 5958 (2020).

## Acknowledgements

The authors appreciate the partial supports of Iran Polymer and Petrochemical Institute and Alzahra University.

## Author contributions

S.S.: Conceptualization; Funding acquisition; Project administration; Resources; Supervision; Writing - review & editing; N.A.-D.: Formal analysis; Data curation; Methodology; Visualization; Investigation; Writing - original draft; M.M.H.: Funding acquisition; Resources; Investigation; Supervision.

## Competing interests

The authors declare no competing interests.

### Additional information

**Supplementary Information** The online version contains supplementary material available at <https://doi.org/10.1038/s41598-022-07708-0>.

**Correspondence** and requests for materials should be addressed to S.S. or M.M.H.

**Reprints and permissions information** is available at [www.nature.com/reprints](http://www.nature.com/reprints).

**Publisher's note** Springer Nature remains neutral with regard to jurisdictional claims in published maps and institutional affiliations.



**Open Access** This article is licensed under a Creative Commons Attribution 4.0 International License, which permits use, sharing, adaptation, distribution and reproduction in any medium or format, as long as you give appropriate credit to the original author(s) and the source, provide a link to the Creative Commons licence, and indicate if changes were made. The images or other third party material in this article are included in the article's Creative Commons licence, unless indicated otherwise in a credit line to the material. If material is not included in the article's Creative Commons licence and your intended use is not permitted by statutory regulation or exceeds the permitted use, you will need to obtain permission directly from the copyright holder. To view a copy of this licence, visit <http://creativecommons.org/licenses/by/4.0/>.

© The Author(s) 2022